

# Assessment of Carbon Dioxide Storage Capacity of Selected Aquifers in ‘J’ Field, West Africa

W. O. Raji<sup>1,2\*</sup>, S. O. Bello<sup>1</sup>, T. O. Adeoye<sup>1</sup>



<sup>1</sup>Department of Geophysics, University of Ilorin, PMB 1515, Ilorin, Nigeria

<sup>2</sup>Department of Earth Sciences, Carleton University, Ottawa, Canada



**ABSTRACT:** A combination of seismic data and petrophysical logs from five wells acquired in ‘J’ Field, Niger Delta, Nigeria, have been analyzed to assess the carbon dioxide (CO<sub>2</sub>) storage potential of some saline aquifers in ‘J’ field. The study aims to evaluate the volume of CO<sub>2</sub> that can be potentially stored in the aquifers and the risk of CO<sub>2</sub> leakages in the storage. The sand aquifers were correlated across the five wells to evaluate their thicknesses and lateral extent. Porosity, permeability, formation water resistivity, and net sand thickness were estimated in the different wells. The Horizons corresponding to the top of the aquifers was mapped, and time and depth structured maps were generated for structural analysis and volumetric estimations. The risk of CO<sub>2</sub> leakages through sealing layers (cap rocks) was evaluated in terms of caprock integrity and pore pressure sealing mechanism. Results of the study showed that four aquifers, namely, L20, N30, M40, and P50, are laterally extensive across the five wells and have thicknesses that range from 14 to 352 m. The individual CO<sub>2</sub> storage capacity of L20, M30, N40, and P50 was estimated to be  $6.97 \times 10^{10}$ ,  $1.48 \times 10^{10}$ ,  $7.78 \times 10^9$  and  $1.49 \times 10^{10}$  tons, respectively. The combined aquifer storage capacity was estimated to be  $1.07 \times 10^{11}$  tons. The sealing layers have low risk of CO<sub>2</sub> leakages. The study concluded that the aquifers have good potential for CO<sub>2</sub> storage and low risk of leakages. The study ranked L20 as the best among the four aquifers.

**KEYWORDS:** Carbon capture and storage; Saline aquifers; Global warming; Petrophysical logs; 3D Seismic data; Niger Delta.

[Received May 30, 2022; Revised Jun. 26, 2022; Accepted Jul. 2, 2022]

Print ISSN: 0189-9546 | Online ISSN: 2437-2110

## I. INTRODUCTION

Emission of gases by large industries, oil refineries, and automobile engines releases a vast amount of CO<sub>2</sub> and other air pollutants to the atmosphere, thereby contributing to the greenhouse gas effect. Globally, about 80% of the greenhouse gas emission is attributed to CO<sub>2</sub> released to the atmosphere from fossil fuel during energy production and consumption (Metz *et al.*, 2006; Bachus, 2015; 2016; Berghout *et al.*, 2019). Despite the global efforts to generate energy from non-fossil fuel sources such as solar and wind, about 80% of the global energy need is still being met from fossil fuel (IEA 2017; EPA 2018). Therefore, there is a need to develop strategies to deal with the negative consequences of the consumption of fossil fuels while maximizing the efforts to increase non-fossil fuel sources of energy. The leading solution to greenhouse gas and consequential global warming is to isolate and store CO<sub>2</sub> away from the atmosphere in a geological storage. Studies that confirmed the safety and reliability of Carbon Capture and Storages and demonstrate the capability of Seismic Tomography for detecting CO<sub>2</sub> leakages in geological formations include Saito *et al.* (2006), Ajo-Franklin *et al.* (2013), Chadwick *et al.* (2014), Chadwick *et al.* (2016), Furre *et al.* (2015), Raji *et al.* (2018) and Raji *et al.* (2021). The new trend in Carbon Capture and Storage, CCS research is to characterize the storage site and quantify the volume of CO<sub>2</sub> that can be stored in some of the geological formations.

CCS is the method of capturing carbon dioxide which would have been released to the atmosphere, converting the CO<sub>2</sub> to a supercritical state, and injecting them into deep geological formations such as depleted oil and gas reservoirs, deep saline aquifers, deep coal seams, and salt caverns, among others. CO<sub>2</sub> storage in a subsurface geological formation requires site characterisation, estimation of the potential storage capacities, and evaluation of the risk of leakages in the geological formation. These three factors are important for the safety of the environment. The prior knowledge of the quantity of CO<sub>2</sub> that can be stored in local fields and the property of the regional geological formation is crucial to the successful execution of CCS projects. Estimation of the volume of CO<sub>2</sub> that can be stored in the saline aquifers in ‘J’ Field, Nigeria, and evaluation of the risk of leakages are the key foci of this paper. To the best of the author’s knowledge, the only published study on CO<sub>2</sub> sequestration potential of saline aquifers in Nigeria is a recent paper by Raji *et al.* (2021). At the same time, this type of studies are important to demonstrate the readiness of Nigeria to comply with the Kyoto Protocol and United Nations Framework Convention on Climate Change and global warming. Furthermore, the 2015 World Bank report showed that Nigeria is rated number 39 on the global ranking of carbon emission from all sources.

Studies by Saito *et al.* (2006), Ajo-Franklin *et al.* (2013), Xu and Lei (2006), Bohm *et al.* (2015) among others have shown that injection of CO<sub>2</sub> into saline water aquifers or hydrocarbon reservoirs can change the seismic velocity of the

\*Corresponding author: lanreraji@unilorin.edu.ng; wasiu.rajii@gmail.com

doi: <http://dx.doi.org/10.4314/njtd.v19i3.4>

reservoirs or aquifers by up to 30%. Seismic velocity tomography can be used to image the velocity changes in the CO<sub>2</sub>-injected geological structures to monitor possible leakages. Raji *et al.* (2018) simulated the time-lapse CO<sub>2</sub> movement in a complex reservoir structure of Marmouzi in Angola. The study showed the capability and effectiveness of Seismic Velocity Tomography for monitoring the movement of CO<sub>2</sub> in stratigraphically complex geological storages. The accurate estimates of CO<sub>2</sub> containment of a sequestration site are critical for determining the life span of a storage site, facility costing, and field planning prior to injection. Saline aquifers, when compared to other geological formations such as oil reservoirs and coal beds in terms of CO<sub>2</sub> storage capacity has the largest storage capacity. This is because some of the aquifers are regional in size and have higher porosities compared to hydrocarbon reservoirs and coal seams. For this reason, saline aquifers are considered as the most abundant geological storage for CO<sub>2</sub> (Tomić *et al.* 2018). This is especially true for Nigeria.

The first project on CO<sub>2</sub> storage in offshore saline aquifer in Europe started in 1996 in Sleipner –Norway. More than 17 Mt. of CO<sub>2</sub> has been injected into the aquifer (I.E.A., 2017). A large project on CO<sub>2</sub> storage in onshore saline aquifer is ongoing in Salah, Algeria and Weyburn, Canada - where over 1 Mt CO<sub>2</sub> is being injected into the aquifers per year (Ajo-franklin and Orr 2009). Unlike in developed world like U.S.A., Australia, Norway, Canada, and Netherlands where there have been extensive published studies on CO<sub>2</sub> storage potentials of subsurface geological media (e.g., Bachus, 2002; Friedman *et al.*, 2005; Solomon, 2007; Kaldi and Gibson-Poole, 2008; Ramirez *et al.*, 2009; Godec *et al.*, 2013; Boyd *et al.*, 2013; Sayer *et al.*, 2013), studies on carbon capture and storage, CCS in Nigerian geologic space are scarcely published. To the best of our knowledge, except (Raji *et al.* 2021), there are no published studies on CO<sub>2</sub> storage potentials of aquifers in Nigeria. However, published research work on CO<sub>2</sub> storage potential and leakage assessment in Nigerian are essential to demonstrate prior knowledge and state of the art for future projects.

Further, recent studies showed that the nature of CO<sub>2</sub>–brine–rock behavior in geosequestration site depends on phase of CO<sub>2</sub>, the mineral composition of the rock, and the age of the storage (Peter *et al.*, 2022). Visco-acoustic modelling of P-and S-waves velocity models of complex structures suitable for CO<sub>2</sub> storage and wavefield separation of complex seismic data are described in Raji (2017) and Raji *et al.* (2019). The future research agenda include large scale storage at GtCO<sub>2</sub>/year and reservoir characterisation from nano to kilometer scales (Kelemen *et al.*, 2019). The current study extended the work of Raji *et al.* (2021) which estimates the volume of CO<sub>2</sub> storable in some saline aquifers in the Niger Delta of Nigeria by including the computation of spatial petrophysical maps of aquifer properties and the assessing the potential of CO<sub>2</sub>

leakages in the cap rocks. The overall aim of this study is to evaluate the volume of CO<sub>2</sub> that can be potentially stored in the aquifers and the risk of CO<sub>2</sub> leakages in them.

## II. GEOLOGY AND STRATIGRAPHY OF THE NIGER DELTA

The study area is located in the Niger Delta Province of Nigeria. A detailed description of the field is not provided for proprietary reasons. The Niger Delta is located between latitude 4° and 6° N, longitude 3° and 9° E (Figure 1). It is formed by a rift basin in relation to the opening of the South Atlantic Ocean. It is one of the largest sub-aerial basins in Africa, covering about 300,000 km<sup>2</sup> with sediment fill of 9 -12 km. The geology of the area originally described by (Short and Stauble, 1967; Doust and Omatsola, 1990) is briefly reviewed in this section. The three main lithostratigraphic units in the Niger Delta are: (i) shale dominated Akata Formation, (ii) the sand dominated Agbada Formation, and (iii) the Benin Formation. Akata formation is the lowest and oldest unit. This formation underlies the entire Niger Delta area having sediment thickness up to 7 km in some places (Doust and Omatsola, 1990). Akata formation's age ranges from Paleocene to recent and it primarily consist of shale, clay and silt. The shale in Akata formation forms the potential source rock. The shale is sufficiently thick and rich in organic matter capable of generating hydrocarbon (Evamy *et al.*, 1978).

Agbada formation overlies the Akata formation and is made of sand and shales of fluvio-marine origin. Agbada is the main hydrocarbon-bearing interval in the Niger Delta (Evamy *et al.*, 1978). The formation is about 3700 m thick, dated Eocene to recent. The Agbada formation forms the hydrocarbon-prospective sequence in the Niger Delta. Most exploration wells in the Niger delta have bottomed in the Agbada formation. Hydrocarbon traps in Agbada formation are formed by stratigraphic traps. In few cases, we have structural traps and a combination of structural and stratigraphic traps. Roll-over anticline, which occurs in front of growth faults, is the main target of hydrocarbon explorationists in the Niger Delta of Nigeria. Agbada formation houses the reservoir, the trap, and the seal. In the exploration sense, the Agbada formation is the most important lithofacies in the Niger Delta petroleum system. (Jibrin and Raji 2014; Adeoye *et al.* 2018).

The Benin formation is the youngest (Oligocene to Recent) and shallowest among the three lithofacies in the Niger Delta. It directly overlies the Agbada formation and consists of coarse-grained to gravelly sandstones. Benin formation hosts the most prolific aquifers in the Niger Delta region of Nigeria. The aquifers range from shallow to intermediate and deep. The deep aquifers in the Benin Formation are the candidate facility for CO<sub>2</sub> storage in this study. The deep aquifers have good internal regional hydraulic connections and are separated by shale layers of significant thickness. These shale layers have characteristic low permeability and porosity to serve as cap rocks for the aquifers and hence made these sand layers good candidates for the storage of CO<sub>2</sub>.

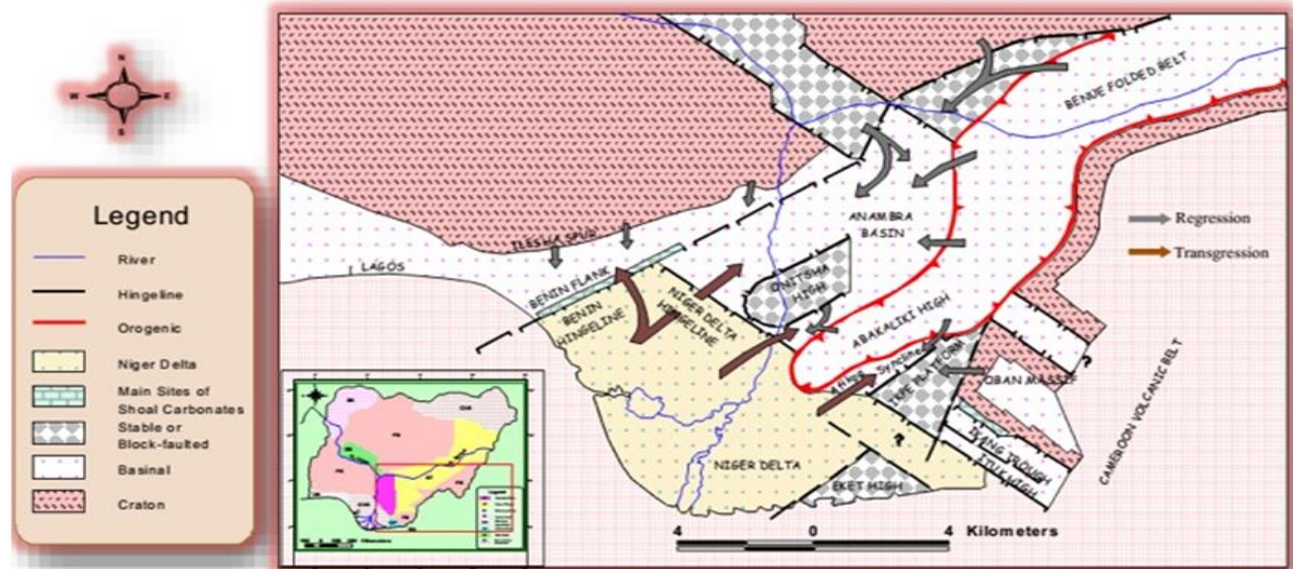


Figure 1: Tectonic Map of Niger Delta, Nigeria. Inset – Map of Nigeria (Evamy et al., 1978).

### III. MATERIALS AND METHOD

#### A. Materials

To estimate the potential CO<sub>2</sub> storage capacity of any geological formation, the evaluation of the area, thickness, porosity, and permeability, among other properties of the formation are required. This information is often derived from well logs and core data. The data used for this study were provided by the Department of Petroleum Resources (DPR), Nigeria. The data set comprised petrophysical logs from five wells and 3D seismic data covering the 'J' Field.

The wells are named Pearl 01, 02, 03, 04, and X01; the welllogs provided include gamma, resistivity, spontaneous potential, and porosity. Core data from the wells were not available for this study. Five thick and laterally extensive saline sand aquifers penetrated by the wells were selected for the study. Seismic and well logs data were evaluated using volumetric approach and Petrel 2009 (by Schlumberger) was used to plot the maps and correlate the aquifers across the wells in the area.

#### B. Evaluation of the Selected Aquifers and Estimation of their Storage Capacity

A combination of gamma-ray and spontaneous potential (SP) log was used to discriminate sand from shale layers using a cut of 70 American Petroleum Institute (API). Then, resistivity logs were used to ascertain that the thick sand aquifers selected were saline aquifers, not freshwater aquifers. The values of the deep resistivity logs were examined at the reservoir intervals and compared to the freshwater resistivity in the same area. The resistivity of fresh water in the Niger Delta is typically greater than 10 Ωm (Oteri, 1987).

The selected aquifers were examined for lateral continuity across the five wells using lithologic correlation. The lithologic

correlation template in Petrel 2009 version was applied to correlate the sand layer in one well to the equivalent sand layer in another well and then across all the five wells. Consequent to the correlation, one of the five sand layers that were initially selected for the study was rejected due to poor lateral continuity. The four sand layers that have good lateral continuity and vertical extent were further evaluated. For references and clarity, the four saline aquifers were named L20, M30, N40, and P50. The gross thicknesses of the saline aquifers were estimated from the logs, and then the net thicknesses Nt. Other petrophysical parameters such as formation water resistivity, hydraulic conductivity, porosity and permeability of the aquifer were also estimated within the aquifer intervals and plotted for spatial correlation.

The 3D seismic volume has been preprocessed for signal enhancement and interpreted to better define the structural framework of 'J' Field. Well-to-seismic tie were performed to determine the horizons that correspond to the top of the saline aquifers on the seismic section. Synthetic seismic data were generated from density and velocity (inverse sonic log) logs using the reflectivity method and Ricker wavelet as the source impulse. Then, the horizons corresponding to the top of the four aquifers, namely, L20, M30, N40, and P50 were picked using seed detection and line-based interpretation strategy. Time-domain structural maps were generated for each aquifer. Then, the time structured maps were converted to their corresponding depth-structured maps using the check shot data. The depth structured map was used to calculate the aquifer surface area required for volumetric estimations, to evaluate the structural framework and the potential trapping mechanism within the aquifers.

The CO<sub>2</sub> storage capacity, G<sub>CO<sub>2</sub></sub> of the individual aquifer was calculated following the method of Bachus (2015) as:

$$G_{CO_2} = A_{av} h_{av} \phi \rho_{CO_2} E (1 - S_w) \quad (1)$$

where:  $A_{Av}$  is the average area of the aquifer,  $h_{av}$  is average thickness of the aquifer,  $\phi$  is the average porosity,  $\rho_{CO_2}$  is the density, E is the storage efficiency factor, and  $S_w$  is the average water saturation.

The density of supercritical CO<sub>2</sub> at depth interval of 1000 to 2500 and temperature of 67oC is 0.54 g/cm<sup>3</sup> (or 540 kg/m<sup>3</sup>). In addition to the storage property and the viscosity of the fluid, the CO<sub>2</sub> storage efficiency, E of an aquifer depend on a combination of four factors described in Bachus (2015). These factors include: (i) the in situ conditions of the aquifer (temperature, pressure, lithology, porosity, permeability, heterogeneity, anisotropy, among others); (ii) characteristics of the confining aquitard or cap-rock (capillary entry pressure and permeability); (iii) characteristics of CO<sub>2</sub> operation – injection rate, duration of injection, number of injection wells and their spacing, and (iv) regulatory constraints – the maximum bottom hole injection pressure, relevant aquifer area, and the scale of assessment – local or regional. The results obtained are presented in Figures 2 to 5 and discussed in Section IV.

C. Evaluation of the Caprocks for Leakages

The caprocks (or seals) covering the aquifers were examined for the possibility of CO<sub>2</sub> leakages. The sealing layers to the aquifers were mapped, their thickness and lateral coverage were evaluated from the well logs. The densities of each of the four sealing layers were plotted against depths following Skerlec’s model (Skelec, 1982) to evaluate the in-situ ductile-brittle behaviour of each sealing layer/cap rocks and to predict their response to pressure. The results obtained are presented in Figures 6a and 6b and discussed in the next sections.

IV. RESULTS AND DISCUSSION

The correlation panel in Figure 2 showed that the selected four saline aquifers are sufficiently thick and laterally continuous across the five wells. This suggests that the aquifers can store a significant quantity of CO<sub>2</sub>.

Further, Figure 2 also shows that saline aquifers are located within a depth range of 910 and 2300 m, which is higher than

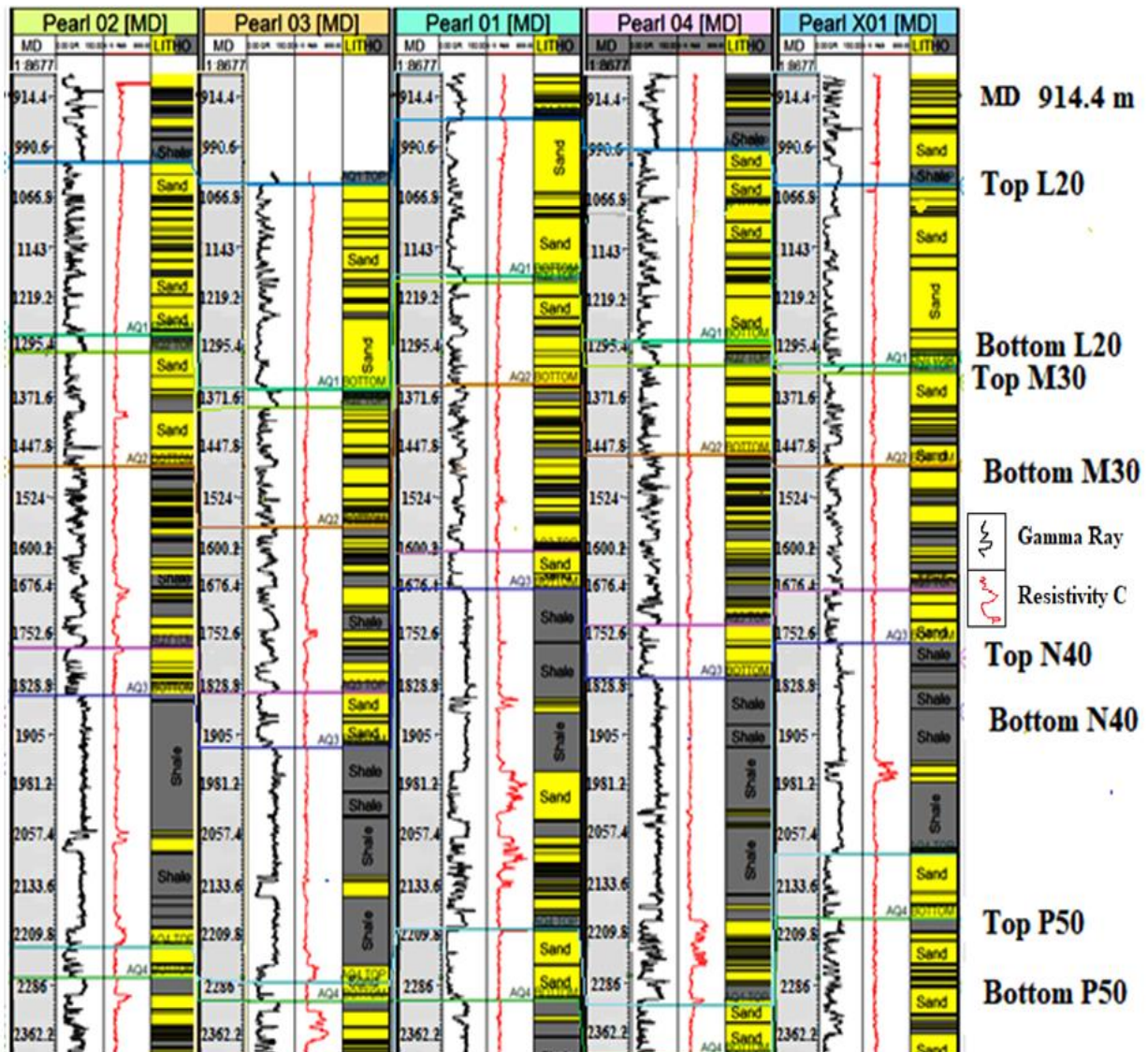


Figure 2. Correlation Panels for the five wells showing the top and bottom of aquifers L20, M30, N40 and P50.

the minimum depth of 800 m required for a CO<sub>2</sub> storage site. The higher the depth, the lower the chance of CO<sub>2</sub> leakage to the atmosphere. Figure 2 also shows the depth sequence of the aquifers, indicated that aquifer L20 is the shallowest, while aquifer P50 is the deepest. The average values of porosity, permeability, hydraulic conductivity, water saturation, formation water resistivity, and aquifer thickness estimated in the aquifer intervals are shown in tables 1-4. Core data for the interval under study are not available, however published data on an adjacent oil field (Etu-Efeotor and Akpokodje, 1990) confirmed the validity of the porosity and permeability data. The porosity and permeability models around the wells are shown in Figure 3.

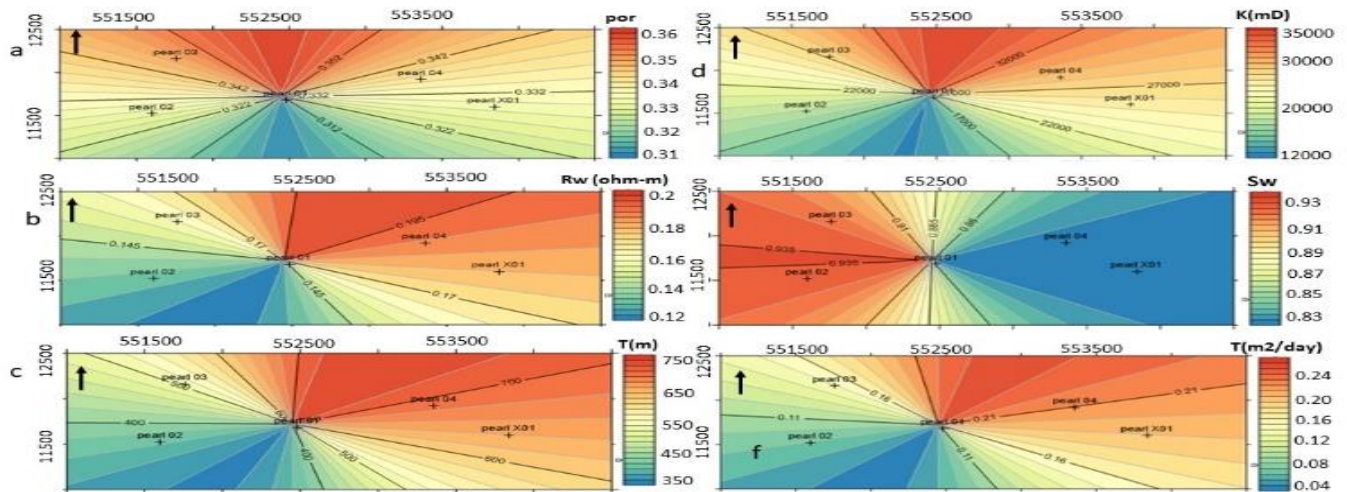


Figure 3: Subsurface maps showing the spatial distribution of some aquifer properties around the five wells.

Porosity and permeability are key parameters in storage and fluid flow, bulk resistivity and formation resistivity are important parameters for predicting the nature of the fluid in the aquifer and the chemical reaction CO<sub>2</sub> may undergo during storage in the aquifers. Water saturation is important for estimating the fraction of the pore space that is readily available for CO<sub>2</sub> storage at in situ condition. When the injection pressure is higher than the pore pressure, the pressure difference can force CO<sub>2</sub> to replace formation water in the pore spaces of the aquifers.

Finer details of the petrophysical parameters of the aquifers, from one well to another, are shown in Tables 1-4. The tables show that the four saline aquifers L20, M30, N40, and P50 have sand thicknesses that ranges from 219 to 277 m, 105 to 147 m, 59 to 79 m, 28 -105 m, respectively. Table 1 also shows that the formation water resistivity is very low - ranging from 0.12 to 0.25  $\Omega$ m, thereby suggesting that the aquifers contain saltwater, not freshwater. The freshwater aquifers in the Niger Delta area have resistivity values greater than 10  $\Omega$ m (Oteri, 1987). The seismic section showing the stratigraphic succession of the saline aquifers is presented in Figure 4. The Horizons corresponding to the tops of the aquifers were picked and some faults were mapped using different colours as shown in Figure 4. The shallowest and deepest horizons correspond to L20 and P50, respectively. The depth maps used for volumetric estimation of CO<sub>2</sub> storage in the aquifers are shown in Figure 5. The maps showed the position of the wells, depths (coded in

colours), and some structural elements such as fault-assisted closures.

The estimated volumes of CO<sub>2</sub> potentially storable in Aquifers L20, M30, N40, and P50 are presented in Table 5, at 1%, 4%, 10% and 15% efficiency factors, respectively. The reason for calculating CO<sub>2</sub> volume at different efficiency factors is that there is no consensus among CO<sub>2</sub> sequestration researchers on the best or the most appropriate efficiency factor to estimating the CO<sub>2</sub> storage potential of aquifers. Also, the efficiency factor depends on a number of factors which are still not completely understood, including the characteristics of the aquifer and the caprock (Bachus, 2015).

The value commonly used in the literature ranges from 1% to 20% (Van der Meer, 1982:1995; Holloway *et al.*, 2006; EERC, 2009). Consequently, the storage potential of aquifers estimated at 1%, 4%, 10%, and 15% are shown in Table 5. Results in Table 5 shows that aquifer L20 has the highest storage capacity at all the efficiency factors, while aquifer P50 has the lowest storage capacity at all the efficiency factors. The total volume of CO<sub>2</sub> that can be stored in the combined aquifer are  $2.78 \times 10^{11}$  tons,  $5.90 \times 10^{11}$  tons,  $3.11 \times 10^{10}$  tons, and  $5.94 \times 10^{10}$  tons at 1%, 4%, 10%, and 15% efficiency factors, respectively. For this study, the average estimated storage capacity of the individual aquifer was computed as the mean of the storage capacities of the respective aquifers at 1%, 4%, 10% and 15% efficiency factors. The average estimated storage capacities of the individual aquifers are  $6.97 \times 10^{10}$  tons,  $1.48 \times 10^{10}$  tons,  $7.78 \times 10^9$  tons and  $1.49 \times 10^{10}$  tons for L20, M30, N40, and P50 aquifers, respectively. The estimated combined aquifer storage capacity, being the sum of the estimated average storage capacity of the four aquifers, is  $1.07 \times 10^{11}$  tons. The estimated volumes are comparable with those obtained in previous studies (Sayers *et al.*, 2015; Kelemen *et al.*, 2019): keeping other factors constant, the thicker the aquifers the higher the CO<sub>2</sub> volume storable in them.

The cap rocks (seals) were found to be laterally extensive, covering the entire aquifer area. Figure 6a shows the estimated thickness of seals 1 - 4 in the different wells, where seals 1, 2, 3, and 4 are the respective seal to aquifers L20, N30, M40, and

**Table 1. Petrophysical parameters of Aquifer L20 across the five wells.**

Well	Top (m)	Base(m)	HT(m)	ST (m)	R ( $\Omega$ m)	K(mD)	$\phi$	Rw( $\Omega$ m)	k (m/day)	Sw
Pearl 02	1013.4	1276.6	263.2	222.5	2.65	31710.4	0.355	0.199	9.8*10 <sup>-4</sup>	0.65
Pearl 03	1047.6	1360.0	312.4	275.5	2.41	28790.6	0.350	0.168	9.7*10 <sup>-4</sup>	0.92
Pearl 01	950.5	1187.0	236.0	219.5	2.45	40703.1	0.369	0.199	9.4*10 <sup>-4</sup>	0.69
Pearl 04	994.8	1299.6	304.8	277.1	2.21	15143.7	0.317	0.256	6.3*10 <sup>-4</sup>	0.95
Pearl X01	1048.7	1322.8	274.1	256.8	1.28	60583.4	0.392	0.237	1.5*10 <sup>-3</sup>	1.0

**Table 2. Petrophysical parameters of aquifer M30 across the five wells.**

Well	Top (m)	Base(m)	HT(m)	ST(m)	Rt ( $\Omega$ m)	K (mD)	$\phi$	Rw ( $\Omega$ m)	k (m/day)	Sw
Pearl 02	1303.4	1475.9	172.5	147.1	1.568	23949.7	0.340	0.166	9.3*10 <sup>-4</sup>	0.817
Pearl 03	1386.6	1568.1	181.5	142.9	0.993	15269.2	0.318	0.122	7.4*10 <sup>-4</sup>	0.946
Pearl 01	1197.4	1352.1	154.7	133.9	1.062	18335.0	0.327	0.131	7.4*10 <sup>-4</sup>	0.920
Pearl 04	1322.8	1459.3	136.7	115.9	1.02	15237.8	0.318	0.130	7.0*10 <sup>-4</sup>	0.966
Pearl X01	1336.0	1474.6	138.5	105.8	0.991	24982.2	0.343	0.151	9.5*10 <sup>-4</sup>	0.974

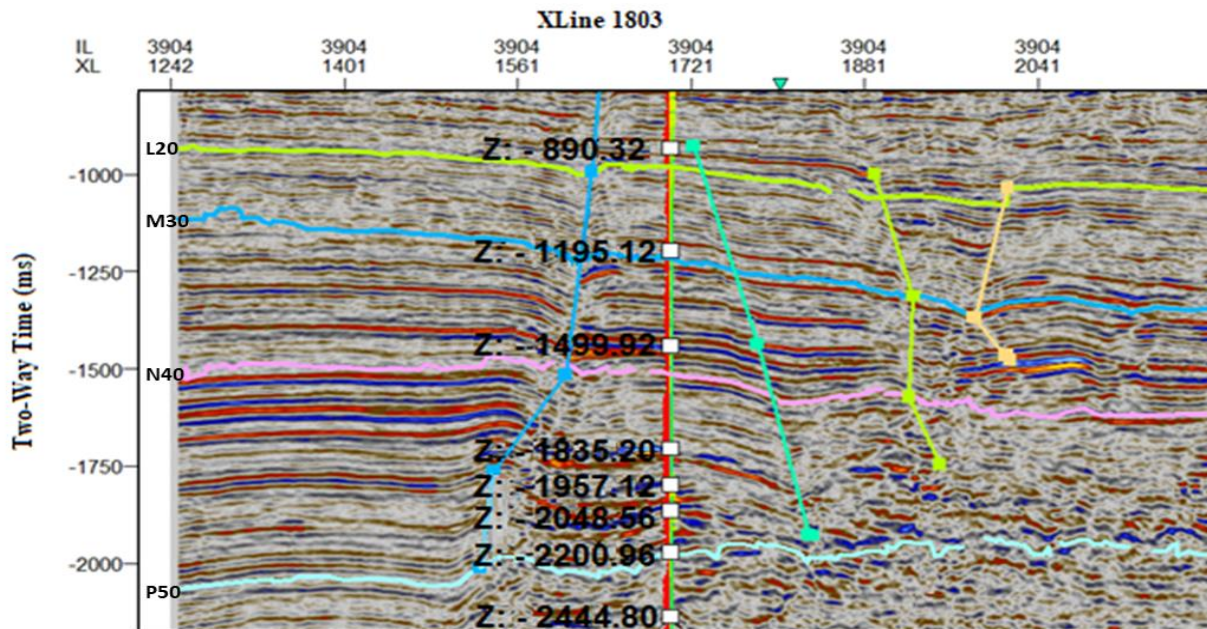
**Table 3. Petrophysical parameters of aquifer N40 across the five wells.**

Well	Top (m)	Base (m)	HT (m)	ST (m)	Rt ( $\Omega$ m)	K (mD)	$\phi$	Rw ( $\Omega$ m)	km/day)	Sw
Pearl 02	1774.2	1845.6	71.4	59.4	1.344	19427.6	0.3296	0.131	9.8*10 <sup>-4</sup>	0.808
Pearl 03	1841.7	1924.8	83.2	74.20	0.829	11814.8	0.3055	0.099	7.5*10 <sup>-4</sup>	0.974
Pearl 01	1605.5	1684.2	78.8	77.3	0.914	5455.02	0.2715	0.089	4.3*10 <sup>-4</sup>	0.998
Pearl 04	1738.1	1820.4	82.3	79.4	0.974	21190.6	0.3340	0.136	1.0*10 <sup>-3</sup>	0.956
Pearl X01	1685.1	1766.8	81.8	75.8	0.976	29224.3	0.3508	0.144	1.2*10 <sup>-3</sup>	0.932

**Table 4. Petrophysical parameters of aquifer P50 across the five wells.**

Well	Top (m)	base(m)	HT(m)	ST (m)	Rt ( $\Omega$ m)	K (mD)	$\phi$	Rw ( $\Omega$ m)	k (m/day)	Sw
Pearl 02	2227.5	2273.4	45.9	41.5	1.14	13195.9	0.311	0.121	9.1 *10 <sup>-4</sup>	0.899
Pearl 03	2281.5	2312.1	30.6	27.8	1.26	4665.9	0.266	0.091	5.1*10 <sup>-4</sup>	0.881
Pearl 01	2201.2	2309.7	108.5	105.6	2.08	8708.9	0.292	0.118	7.3*10 <sup>-4</sup>	0.706
Pearl 04	2316.8	2393.1	76.3	71.86	1.77	4462.4	0.263	0.117	5.1*10 <sup>-4</sup>	0.850
Pearl X01	2089.1	2185.6	96.6	92.2	1.37	5363.6	0.271	0.110	5.3*10 <sup>-4</sup>	0.913

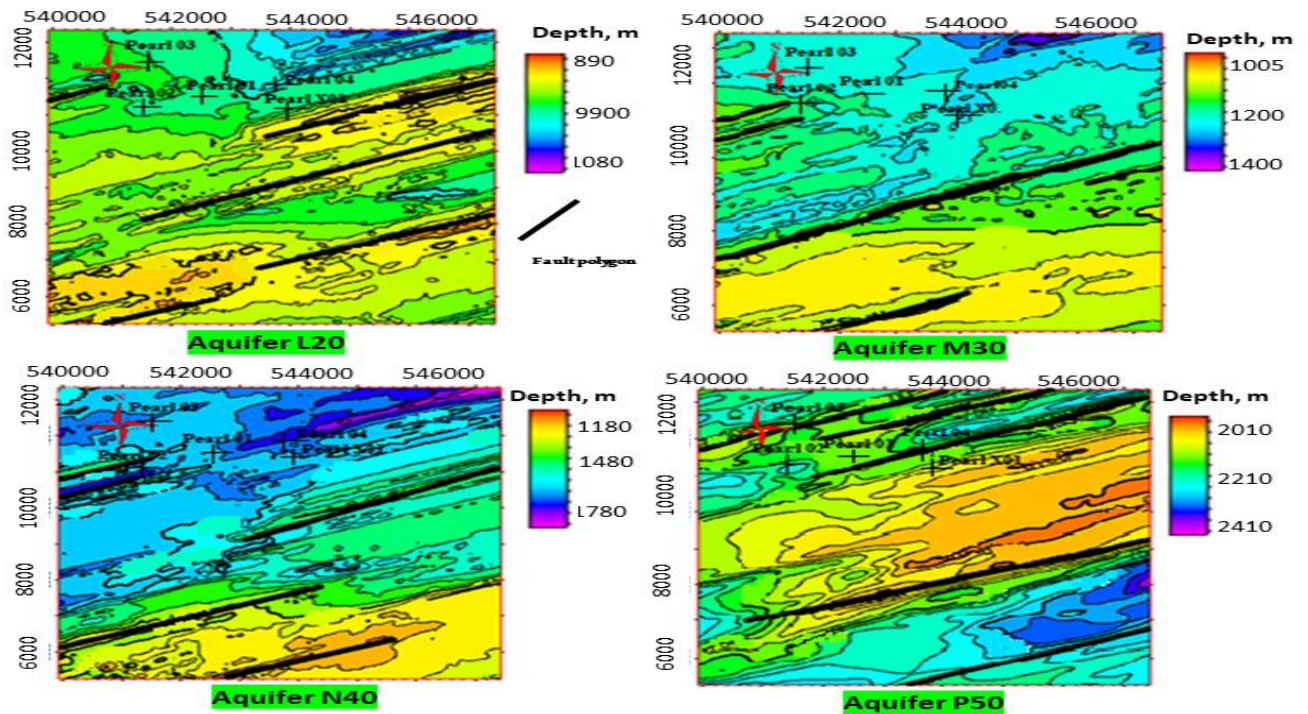
HT = Horizon Thickness (ft), ST = Sand Thickness (ft), Rt = True resistivity of formation (( $\Omega$ m), K= Permeability (mD),  $\phi$  = average Porosity, Rw = Resistivity of formation water (( $\Omega$ m),k = Hydraulic Conductivity (m/day), Sw= Water Saturation.



**Figure 4: Seismic section showing cross line 1803, the horizons picked and some fault lines.**

**Table 5: Estimated CO<sub>2</sub> storage capacities of the individual and combined aquifer.**

	L20 Storage Capacity	M30 Storage Capacity	M40 Storage Capacity	P50 Storage Capacity	Combined storage capacity of aquifer
CO <sub>2</sub> storage at 1% Efficiency Factor	9.61x10 <sup>9</sup>	2.03x10 <sup>9</sup>	1.07x10 <sup>9</sup>	2.06x10 <sup>9</sup>	2.78x10 <sup>11</sup>
CO <sub>2</sub> storage at 4% Efficiency Factor	3.88x10 <sup>10</sup>	8.14x10 <sup>9</sup>	4.30x10 <sup>9</sup>	8.25x10 <sup>9</sup>	5.90x10 <sup>11</sup>
CO <sub>2</sub> storage at 10% Efficiency Factor	9.61x10 <sup>10</sup>	2.03x10 <sup>10</sup>	1.07x10 <sup>10</sup>	2.06x10 <sup>10</sup>	3.11x10 <sup>10</sup>
CO <sub>2</sub> storage at 15% Efficiency Factor	1.35x10 <sup>11</sup>	2.84x10 <sup>11</sup>	1.52x10 <sup>10</sup>	2.88x10 <sup>10</sup>	5.97x10 <sup>10</sup>
The storage capacity of the aquifer at the average of 1, 4, 10, & 15% E. F	6.97x10 <sup>10</sup>	1.48x10 <sup>10</sup>	7.78x10 <sup>9</sup>	1.48x10 <sup>10</sup>	1.07x10 <sup>11</sup>

**Figure 5: Depth structured maps of saline aquifers: top left L20 aquifer; top right- M30 aquifer; Bottom left - N40 aquifer; and bottom right -P50 aquifer.**

P50. The thicknesses of the seal (Figure 6a) ranges from 14 to 352 m which are above the minimum. The minimum seal thickness required for CO<sub>2</sub> sequestration is 10 m (Kaldi *et al.*, 2008). Seal 4 is consistently the thickest in all the wells, while seal 1 is the second thickest. The thicker the seal, the lower the risk of CO<sub>2</sub> leakage due to breakage or diffusion. Using Skerlec (1982) model to assess the brittle-ductile behaviour of the cap rocks (seals), Figure 6b shows that all the cap rocks plotted in the lower part of the ductile section within the density values of 2.0 to 2.35 g/cm<sup>3</sup>, at depth range of 910 to 2300 m. This result suggests that the seals are moderately ductile and have a low risk of breakage. Ductility in shale is a function of the compaction state; the more the ductility, the lower the risk of breakage. Overall, Aquifer L20 has the highest storage capacity, and its seal has the second-best rating. Therefore, it is rated as the best aquifer in terms of CO<sub>2</sub> storage and risk of leakage.

Compacted low-density shale layers are very ductile, while a high density un-compacted shale layers are usually brittle. The

ductility of the caprock allows it to deform without developing high permeability pathways for leakages. Redox reaction and carbonate precipitation in caprocks can further reduce CO<sub>2</sub> diffusion when there are no large permeability features (Wang and Tokunaga, 2015).

Considering a density range of 1.2 to 2.8 g/cm<sup>3</sup> within a depth range of 100 – 5000 m according to Skerlec's model and the result in Figure 6b where the seal (shale) plotted at the medium density values of 2 to 2.35 g/cm<sup>3</sup> within a depth range of 910 to 2300 m. The seals are interpreted to be moderately ductile. Therefore, the seals have a low risk of breakage and CO<sub>2</sub> leakages. Further, the depth structured map shown in Figure 5 revealed the presence of fault assisted closures that are potentially useful for CO<sub>2</sub> trapping within the aquifers.

Considering capillary pressure and the trapping mechanism for CO<sub>2</sub> in storage media, capillary pressure generally serves as either a driving or opposing force for CO<sub>2</sub> leakages through the sealing layer depending on the prevailing condition and the

property of the storage formation especially in the cap rock transition zone. As seen in the log signatures, porosity heterogeneity at the aquifer - cap rock (seal) transition zone will lead to residual trapping of CO<sub>2</sub> in the cap rock, and this would play a major role in opposing CO<sub>2</sub> leakages in the cap rock (see also, Al-Menhali and Krevor, 2016). Solubility trapping of CO<sub>2</sub> is also possible due to the presence of brine in pore spaces of the media. However, core sample analyses are required to describe the detailed trapping mechanisms. Further, the presence of interbedded layers of shale and sand at the top and base of the storage media will cause significant porosity heterogeneity at the top and base of the aquifers. The heterogeneity will limit the capillary pressure driving CO<sub>2</sub> migration in the caprock. Furthermore, the stratigraphic traps caused by porosity heterogeneity can store significant CO<sub>2</sub> volume, block the pores in the zones, and further reduce the chance of CO<sub>2</sub> leaking through the cap rock.

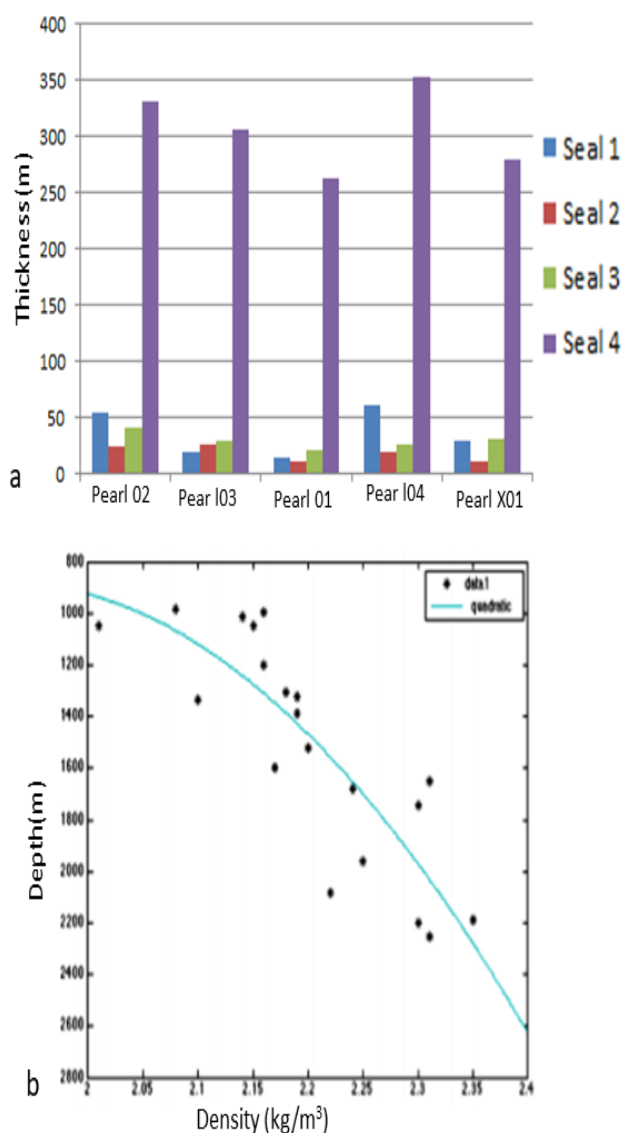


Figure 6 (Top) Plot of bulk density versus depth –using Skerlec’s (1982) model to evaluate risk of breakage in seal/ cap rock. (Bottom) histogram showing the estimated thickness of the seal/cap rock in the five wells (bottom).

## V. CONCLUSION

The volume of CO<sub>2</sub> that can be stored in the saline aquifers in 'J' Field Niger Delta, Nigeria, has been estimated. Furthermore, the risk of CO<sub>2</sub> leakages through the cap rocks overlying the aquifers has been evaluated. The aquifers were found to be sufficiently thick and laterally extensive to store a significant volume of CO<sub>2</sub>. The storage capacity of the combined aquifers was estimated to be  $1.07 \times 10^{11}$  tons, while the individual storage capacity of L20, M30, N40, and P50 aquifers are  $6.97 \times 10^{10}$  tons,  $1.48 \times 10^{10}$  tons,  $7.78 \times 10^9$  tons and  $1.49 \times 10^{10}$  tons, respectively. The caprocks (seals) are formed by shale that are moderately ductile, sufficiently thick, and laterally extensive, covering the entire surface area of the respective aquifers to be used for storage. Aquifer L20 has the highest storage capacity, and its seal has the second-best rating.

Aquifer P50 has the best sealing layer and the least storage capacity. In terms of storage capacity and the risk of leakages, aquifer L20 is rated as the best. The stratigraphic succession of the selected aquifers made it possible for the aquifers to be sandwiched between the competent top and bottom shale layers, which further reduced the risk of CO<sub>2</sub> leakages. The study concludes that aquifers L20, M30, N40 and P50 are good and reliable for safe and secure storage of CO<sub>2</sub> in J field. Findings from this study are important for basin-wide evaluation of CO<sub>2</sub> storage in Nigerian geological space in the mitigation of greenhouse gas effect. Similar studies on depleted hydrocarbon reservoirs in the Niger Delta of Nigeria is recommended with a view to prepare a template for a pilot study.

## ACKNOWLEDGEMENTS

The authors thankfully acknowledge the reviewers for their helpful comments and suggestions. The authors are grateful to the Department of Petroleum Resources for the release of the data used for this study.

## DECLARATION

Funding: No funding was received for this study.

*Conflict of interest:* to the best of authors’ knowledge, there is no known conflict of interest in this study and the manuscript.

*Data availability:* The data is not available to the public due to proprietary reason.

## REFERENCES

- Adeoye, T.O and Raji, W. O. (2018). Hydrocarbon Reserve Estimation and Risks Assessment in X-ray Field, Niger Delta, Nigeria. Adamawa State University Journal of Scientific Research, 6:32-45.
- Ajo-Franklin, J.B.; J. Peterson; J. Doetsch and T. M. Daley (2013). High resolution characterization of a CO<sub>2</sub> plume using crosswell seismic tomography: Cranfield, MS, USA. Int. J. Greenhouse Gas Control 18: 497–509.
- Al-Menhali, A.S. and Krevor S. (2016). Capillary Trapping of CO<sub>2</sub> in Oil Reservoirs: Observations in a Mixed-Wet Carbonate Rock. Environ. Sci. Technol. 2016, 50, 5, 2727–2734.
- Bachus, S. (2002). Sequestration of CO<sub>2</sub> in geological media in response to climate change: road map for site selection using the transform of the geological space into the

CO<sub>2</sub> phase space. *Energy Conversion & Management*, 43: 87-102.

**Bachus, S. (2015).** Review of CO<sub>2</sub> storage efficiency in deep saline aquifers. *International Journal of Greenhouse Gas Control* 40 (2015) 188–202.

**Bachu, S. (2016).** Identification of oil reservoirs suitable for CO<sub>2</sub>-EOR and CO<sub>2</sub> storage (CCUS) using reserves databases, with application to Alberta, Canada. *Int. J. Greenhouse Gas Control* 44: 152–165. <https://doi.org/10.1016/j.ijggc.2015.11.013>.

**Berghout, N.; H. Meerman; M. Van den Broek and A. Faaij (2019).** Assessing deployment pathways for greenhouse gas emissions reductions in an industrial plant – a case study for a complex oil refinery. *Appl. Energy* 236: 354–378. <https://doi.org/10.1016/j.apenergy.2018.11.074>.

**Böhm, B.; J. M. Carcione; D. Gei; S. Picotti and A. Michelini. (2015).** Cross-well seismic and electromagnetic tomography for CO<sub>2</sub> detection and monitoring in a saline aquifer, *Journal of Petroleum Science and Engineering*, 133: 245-257 doi:10.1016/j.petrol.2015.06.010.

**Boyd, A. D.; Y. Liu; J. C. Stephen; E. J. Wilson; P. Melisa; T. R. Peterson; E. Einsjedel and J. Meadowcroft. (2013).** Controversy in technology innovation: Contrasting media and expert risk perceptions of the alleged leakage at the Weyburn carbon dioxide storage demonstration project, *International Journal of Greenhouse Gas Control* 14:259-269.

**Chadwick, R. A.; M. Y. Marchant and G. A. Williams. (2014).** CO<sub>2</sub> storage monitoring: Leakage detection and measurement in subsurface volumes from 3D seismic data at Sleipner. *Energy Procedia* 63: 4224–4239.

**Chadwick, R. A.; G. A. Williams and J. C. White. (2016).** High-resolution imaging and characterization of a CO<sub>2</sub> layer at the Sleipner CO<sub>2</sub> storage operation, North Sea using time-lapse seismics. *First Break*, 34(1):77–85.

**Doust, H. and Omatsola, E. (1990).** Niger Delta. In: *Divergent/Passive Margin Basins*. in Edwards, J. D. and P.A. Santogrossi (Eds.), AAPG Memoir, 48:239-248.

**EERC Energy and Environmental Research Center (2009)** Web accessed 19 August 2019, <http://www.undeerc.org/>

**EPA (2018).** United States Environmental Protection Agency. Available from: <https://www.epa.gov/ghgemissions/overview-greenhouse-gases>. Accessed 10/06/2019.

**Etu-Efeotor, J. O. and Akpokodje, E. G. (1990).** Aquifer Systems of the Niger Delta. *Journal of Mining and Geology*. 26(2), 279 – 284.

**Evamy, B. D.; J. Haremboure; P. Kamerling; W. A. Knaap; F. A. Molloy and P. H. Rowlands. (1978).** Hydrocarbon habitat of Tertiary Niger Delta: American Association of Petroleum Geologists Bulletin, 62:1-39.

**Franklin, M. and Orr, J. R. (2009).** CO<sub>2</sub> capture and storage: are we ready? *Energy & Environmental Science*, 2:449-458.

**Friedman, S. J.; J. J. Dooley; H. Held and O. Edenhofer. (2005).** The Low Cost of Geological Assessment for Underground CO<sub>2</sub> Storage: Policy and Economic Implications. *Energy Conversion and Management*, 47:1894-1901.

**Furre, A. K.; A. Kiær and O. Eiken (2015).** CO<sub>2</sub>-induced seismic time shifts at Sleipner. *Interpretation*, 3(3): SS23–SS35.

**Godec, M.; G. Koperna; R. Petrusak and A. Oudinot. (2013).** Assessment of Factors Influencing CO<sub>2</sub> Storage Capacity and Injectivity in Eastern U.S. Gas Shales. *Energy Procedia*, 37:6644-6655.

**IEA (2017)** Key World Energy Statistics. IEA International Energy Agency <https://doi.org/10.1017/CBO9781107415324.004>. accessed on August 21, 2021.

**Jibrin, B. and Raji, W. O. (2014).** Fault detection using dip-steered multi-trace similarity extraction techniques: A case study using offshore Niger Delta 3D Seismic Data. *Journal of Seismic Exploration*. 23: 19-30.

**Kaldi, J. G. and Gibson-Poole, C. M. (2008).** Storage Capacity Estimation, Site Selection and Characterization for Carbon Dioxide Storage Projects. CO<sub>2</sub> CRC, Canberra, Australia. Report No: RPT08-1001.

**Kelemen P.; S. M. Benson; H. Pilorgé; P Psarras, J. Wilcox. (2019).** An Overview of the Status and Challenges of CO<sub>2</sub> Storage in Minerals and Geological Formations, *Frontiers in Climate*, Vol.1, doi.org/10.3389/fclim.2019.00009

**Metz, B.; O. Davidson and H. Coninck. (2006).** IPCC Special Report on Carbon Dioxide Capture and Storage. Cambridge University Press.

**Oteri, A. U. (1987).** Electric logs interpretation for the evaluation of saltwater intrusion in the eastern Niger Delta. *Hydrogeological Sciences Journal*, 33: 19-30.

**Peter, A.; D. Yang; K. I. Eshiet and Y. A. Sheng. (2022).** Review of the Studies on CO<sub>2</sub>–Brine–Rock Interaction in Geological Storage Process. *Geosciences* 2022, 12, 168.

**Raji, W. O. and Rietbrock, A. (2013).** Attenuation estimation in reflection seismic records. *Journal of geophysics and Engineering*, 10(4), 045012.

**Raji, W. O. (2017).** Elastic Velocity Models of a Stratigraphically Complex Carbonate Reservoir, Midland Basin. *Nigerian Journal of Mining and Geosciences*. Vol. 53(1), 1 – 9.

**Raji, W. O.; J. M. Harris and S. Lu. (2018).** Seismic velocity tomography for CO<sub>2</sub> monitor in subsurface geological structures. *Journal of King Saud University-Science*. 28(5) <http://dx.doi.org/10.1016/j.jksus.2016.10.006>

**Raji, W. O.; T. O. Adeoye; K. O. Ibrahim and J. M. Harris. (2019).** Wavefield Separation for Shear Wave Reflections Enhancement. *Nigerian Journal of Technological Research*, 14(3), 66 -77.

**Raji, W. O.; S. O. Bello and T. A. Adeoye. (2021).** Evaluation of CO<sub>2</sub> Storage Capacity of Saline Aquifers in OSCAR Field, Niger Delta, Nigeria, extended abstract, 83<sup>rd</sup> international conference of the Society of Exploration Geophysicist, U.S.A., 2021.

**Ramírez, A.; S. Hagedoorn; L. Kramers; T. Wildenborg and C. Hendricks. (2009).** Screening Carbon Dioxide storage options in the Netherlands. *International Journal of Greenhouse Gas Control*. 4(2): 367 – 380.

**Saito, H.; D. Nobuoka; H. Azuma; Z. Xue and D. Tanase. (2006).** Timelapse crosswell seismic tomography for

monitoring injected CO<sub>2</sub> in an onshore aquifer, Nagaoka, Japan. *Exploration Geophysics*, 37(1): 30–36.

**Sayers, J.; C. Marsh; A. Scot; Y. Cinar; J. Bradshaw; A. Hennig; S. Barclay and R. Daniel. (2013)** Assessment of a potential storage site for carbon dioxide: A case study, Southeast Queensland, Australia. *Environmental Geosciences*, 13(2):123-142.

**Skerlec, M. G. (1982).** Treatise of Petroleum Geology / Handbook of Petroleum Geology: Exploring for Oil and Gas Traps, American Association of Petroleum Geologists, 10:10-94.

**Short, K. C. and Stauble, A. J. (1967).** Outline of the Geology of the Niger Delta. *AAPG Bulletin*. 51: 761 –779.

**Solomon, S. (2007).** Carbon Dioxide Storage: Geological Security and Environmental Issues –Case Study on the Sleipner Gas Field in Norway. Bellona Report 128.

**Tomić, L.; V. Karović- Maričić; D. Danilović and M. Crnogorac. (2018).** Criteria for CO<sub>2</sub> storage in Geological formations. *Underground Mining Engineering*, University of Belgrade-Faculty of Mining and Geology, 32: 61-74.

**Xue Z, Lei, X. (2006).** Laboratory study of CO<sub>2</sub> migration in water-saturated anisotropic sandstone, based on P-wave velocity imaging. *Exploration Geophysics*, 37:10–18.

**Xue, Z.; D. Tanase and J. Watanabe. (2006).** Estimation of CO<sub>2</sub> saturation from time-lapse CO<sub>2</sub> well logging in an onshore Aquifer, Nagaoka, Japan. *Exploration Geophysics*, 37, 19–29.

**Van der Meer, L. G. H. (1982).** Investigation regarding the storage of carbon dioxide in aquifers in the Netherlands: *Energy Conversion and Management*, 33(5-8):611-618.

**Van der Meer, L. G. H. (1995).** The CO<sub>2</sub> storage efficiency of aquifers: *Energy Conversion and Management*, 36(6-9): 513-518.

**Wang, S. and Tokunaga, T. (2015).** Capillary Pressure–Saturation Relations for Supercritical CO<sub>2</sub> and Brine in Limestone/Dolomite Sands: Implications for Geologic Carbon Sequestration in Carbonate Reservoirs. *Journal of Environmental Technology*. 49, 7208–7217.

**World Bank (2015).** World Development Indicator. Available online at [data.worldbank.org/country/Nigeria](http://data.worldbank.org/country/Nigeria). Accessed 12th November 2019.